DEFORMATION DUE TO MAGMA MOVEMENT AND ICE UNLOADING AT KATLA VOLCANO, ICELAND, DETECTED BY PERSISTENT SCATTERER INSAR

Andrew Hooper and Rikke Pedersen

Nordic Volcanological Center, Institute of Earth Sciences, University of Iceland, Reykjavik, Iceland

ABSTRACT

Katla volcano is situated in the south of Iceland, and is largely covered by the Mýrdalsjökull ice cap. Historically, Katla is one of the most active of Iceland's volcanoes, with 20 eruptions in the last 1100 years, the last one being in 1918. The proximity of populated areas and international flight paths makes prediction of the timing and character of any future eruption particularly important. Between late 2000 and early 2005 there was increased seismicity beneath the caldera and west flank of Katla, accompanied by upwards and radially outwards movement of two continuous GPS stations north of Katla caldera. This motion has since ceased, but two continuous GPS sites on the southern flank have been trending upwards and south-southwest since 2000, and this motion continues to the present.

We use both persistent scatterer and combined multiple acquisition InSAR techniques to analyse ENVISAT ASAR data acquired from September 2003 to July 2006, and ERS data acquired between 1995 and 2003, to determine line-of-sight displacements for the area surrounding Katla. The signal we see is consistent with a response to ice unloading, and intrusion of magma or fluids is not required to explain the data. We don't, however, rule out shallow intrusion beneath the caldera causing local deformation that is not visible on the volcano flanks. We also identify possible local landsliding occurring on the volcano flanks.

Key words: InSAR; Persistent Scatterer; Small Baseline; Phase Unwrapping; Katla.

1. INTRODUCTION

Katla volcano is situated in the south of Iceland, at the southern end of the Eastern Volcanic Zone (Figure 1). Most of the upper regions of the volcano, including the caldera, are covered by the Mýrdalsjökull ice cap. Katla is abutted on the west flank by Eyjafjallajökull volcano. Historically, Katla is one of the most active of Iceland's volcanoes, with 20 major eruptions in the last 1100 years, the last one being in 1918 [2]. Eyjafjallajökull volcano is also active and experienced recent intrusive episodes in 1994 and in 1999 to 2000 [3]. The proximity of populated areas and international flight paths makes prediction of the timing and character of any future eruption particularly important.

In July 1999, following bursts of low-frequency seismic tremor, a jökulhlaup was released [4, 5]. The subsequent formation of an ice cauldron implies that the jökulhlaup was caused by a subglacial eruption [5, 6]. Between late 2000 and early 2005 there was a moderate increase in seismicity rate beneath Katla caldera, and a much greater increase in seismicity rate in the Goðabunga area, on the west flank of Katla. The increase in seismicity was approximately coincident with upwards and radially outwards movement of two campaign GPS stations north of Katla caldera [7]. This motion has since ceased, but two continuous GPS sites on the southern flank have been trending upwards and south-southwest, after subtraction of plate-spreading motion, since installation in 2000 [8], and this motion continues to the present.

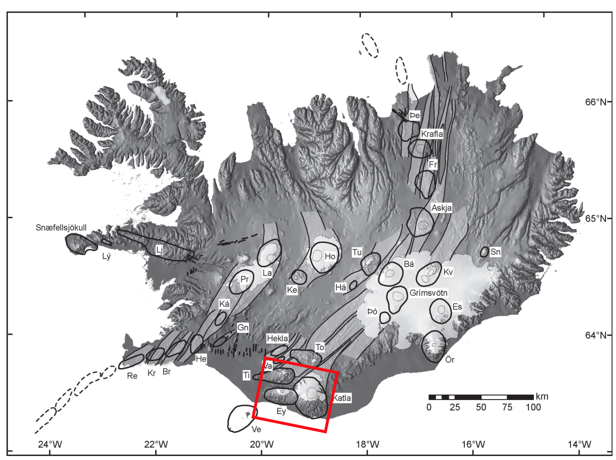

Figure 1. Location of region for which we processed data in Iceland. Katla Volcano is the large volcano on the east side of the processed region and Eyjafjallajökull Volcano is the smaller volcano abutting the west flank of Katla. Background image shows volcanic systems in Iceland plotted on topography in shaded relief, modified from [1].

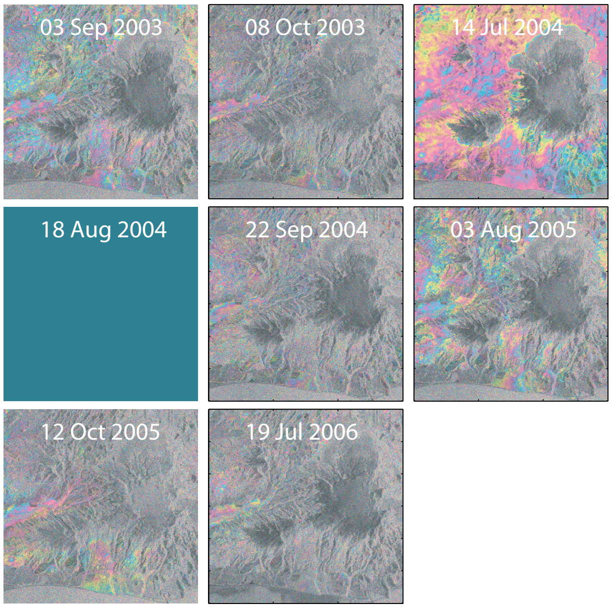

Figure 2. Wrapped interferograms in radar coordinates formed from descending track 324 data acquired by ASAR over Katla, with 4 looks taken in range and 20 in azimuth. The "master" acquisition date is 18 Aug 2004. Each color fringe represents 2.8 cm of displacement in the line-of-sight and the intensity reflects interferogram amplitude.

Crustal deformation occurs in the region of Katla due to tectonic motion related to rifting, thinning of Mýrdasjökull and other icecaps, landsliding, and movement of magma/volcanic fluids. In order to differentiate between these different processes it is essential to have displacement measurements at many points on all sides of the ice cap and at various distances. Currently, there are only three continuous GPS stations operating to the south of Mýrdalsjökull and none to the north. There are also infrequent measurments from campaign GPS benchmarks and optical leveling tilt stations [3]. The spatial density of measurements from InSAR on the other hand is extremely high; however, until now problems associated with noise due to the change in atmospheric delay between satellite passes and inaccuracy in digital elevation models (DEMs) for the area, have made it possible to detect only large signals associated with magma movement in neighbouring Eyjafjallajökull volcano [9, 10]. Smaller signals, such as those expected due to snow and ice mass balance changes, are not detectable above the noise. Furthermore, most ERS-2 data since 2000 are not useable and very few acquisitions have been made by ENVISAT-ASAR, since it started operating in 2003.

Recently, techniques have been developed that are able to estimate atmospheric phase and errors in DEMs, as well as overcome problems of decorrelation, by processing multiple acquisitions together. There are two broad categories of approach: persistent scatterer (PS) and small baseline. Here we use the PS approach developed by Hooper et al. [11] which is applicable when only a few images are avaiable (in this case eight) and when deformation is non-steady. We have enhanced the method by the addition of a new three-dimensional phase unwrapping algorithm based on statistical cost functions. We also implement a combined multiple acquisition method incorporating both PS and small baseline approaches, to maximise the area with useful signal [14]. This method operates on the data at the highest possible resolution and also incorporates three-dimensional phase unwrapping.

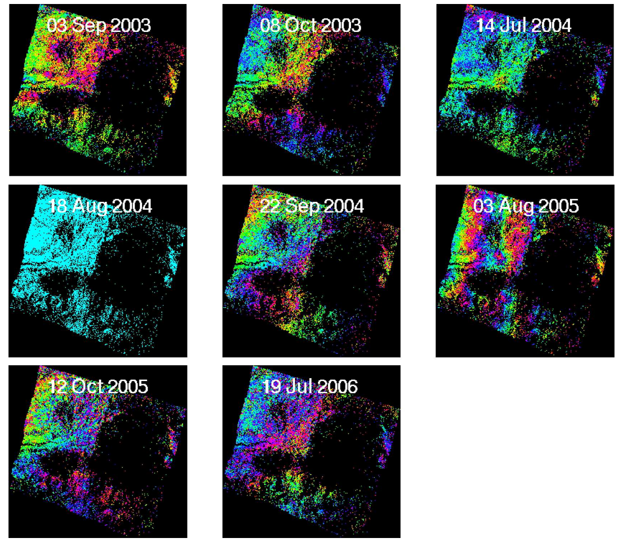

Figure 3. Wrapped phase of persistent scatterer pixels identified in ASAR descending track 324, after correction for look angle error and common-mode atmospheric delay and orbit error. Each color firinge represents 2.8 cm of line-of-sight displacement.

2. DEFORMATION 2003 TO 2006

Although ASAR Swath IS2 data are requested routinely over Katla between May and October, which are generally the snow free months, there have been many cancellations. The most snow-free images of Katla that exist for any descending track is, therefore, only eight, for track 324 and frame 2313.

We formed seven interferograms relative to our chosen "master" scene of 18 August, 2004 (Figure 2). To remove topography we used the 25m posting digital elevation model of the National Land Survey of Iceland. We analysed the resulting interferometric phase using the PS method of Hooper et al. [11]. In this method, pixel phase is adjusted for contributions due to geometry and spatially-correlated terms, and pixels are selected based on the correlation of their adjusted phase with the perpendicular baseline separation of satellite position. This correlation exists because the phase due to error in estimated look angle is proportional to perpendicular baseline. The wrapped phase of the PS pixels selected is shown in Figure 3.

Persistent scatterer analysis becomes increasingly difficult with fewer images, as there is a greater chance that pixels with random phase will fit the model of variation with perpendicular baseline by chance. However, as long as true PS pixels are unwrapped correctly, the presence of pixels with random phase adds only noise to the overall deformation field. Reliable phase unwrapping is then essential. Two algorithms for three-dimensional phase unwrapping of InSAR time series were presented by Hooper et al. [12]. We have improved on these algorithms by extending the two-dimensional statistical cost algorithm of Chen [13] to apply to InSAR time series. Phase differences between neighbouring PS pixels are first smoothed and unwrapped in time to estimate probability distributions of the unwrapped phase difference for each pixel-pair in every interferogram. The probability of any unwrapped solution can then be assessed, and a cost allocated which is equal to the negative of the log of the probability, i.e.,

$$Cost = -log(P) \quad (1)$$

where P is the probability. We use network methods to find approximate minimum-cost solutions in the two spatial dimensions in a similar way to Chen [13], except that we form network by Delaunay triangulation rather than using a grid.

The method of Hooper et al. [11] estimates the spatially-uncorrelated look angle error of PS pixels prior to phase unwrapping, but spatially correlated look angle error, which is present due to spatially correlated errors in the DEM, is only estimated after unwrapping. In the case of large DEM errors and large baselines, however, this contribution can cause the phase to be unwrapped incorrectly. We adopt here an iterative approach to phase unwrapping. First we only unwrap the phase of PS interferograms with the smallest perpendicular baselines. Next we estimate the spatially-correlated look angle error for every PS pixel, relative to an arbitrary reference PS pixel, by finding the best-fitting phase to perpendicular baseline slope in the unwrapped interferograms. Simultaneously we estimate the "master" contribution to the phase due to atmospheric path delay and error in orbit determination, which is given by the zero baseline intersect. We then adjust the wrapped phase of all interferograms from these estimates and unwrap again, this time including larger perpendicular baselines. We iterate around this process until all images are unwrapped, refining the estimates of look angle error and "master" atmospheric and orbit error phase in each iteration.

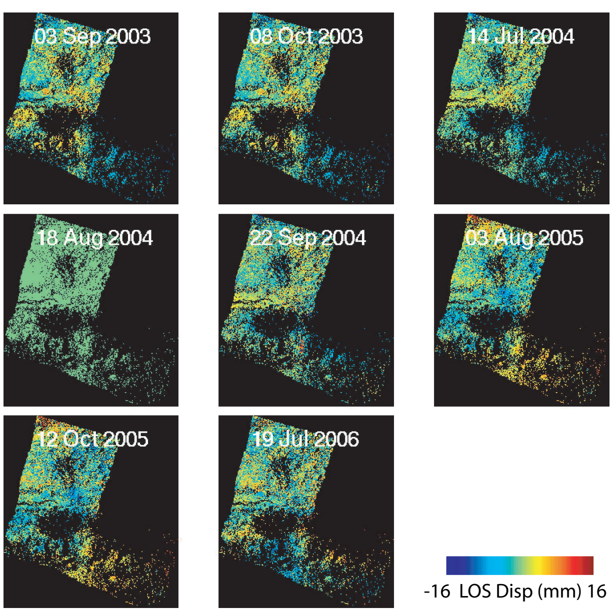

Figure 4. Unwrapped phase of persistent scatterer pixels identified in ASAR descending track 324, after correction for atmospheric delay and orbit error and converted into line-of-sight displacement.

The results of phase unwrapping are shown in Figure 4. The northeast part of the image did not unwrap reliably and is not shown. The contributions of the "slave" images to atmospheric and orbit error phase has also been estimated and subtracted. The results imply that no significant deformation occurred on the flanks of Katla during the period from September 2003 to July 2006.

3. DEFORMATION 2000 TO 2003

This time interval includes most of the period of increased seismicity rates in the caldera and in the Goðabunga region. This interval also includes the movement of two campaign GPS stations, located on nunataks to the north of Katla caldera, upwards and radially outwards relative to a station located at the western end of Eyjafjallajökull [7]. Sturkell et al. [7] propose an inflationary source to explain this deformation, but the sparsity of the GPS network means that the spatial extent of the deformation cannot be well constrained by GPS alone. In particular, it is not known from GPS whether any deformation occurred in the vicinity of Goðabunga.

We processed 27 images acquired by ERS-1/2 in track 324 using the PS method of Hooper et al. [11] as above. All except one of the images were acquired in 2000 or before, and one was acquired in October 2003. The unwrapped phase between September 2000 and this acquisition is shown in Figure 5. Because the last image is isolated in time we are not able to estimate the atmospheric contribution by filtering in time and space. Look angle error has, however, been removed. We find PS pixels in the Goðabunga region, and their phase implies that there was no significant systematic deformation in this region during this period. We don't, however, rule out a shallow intrusion beneath the caldera, as proposed by Sturkell et al. [7], that causes only local deformation, not visible on the volcano flanks.

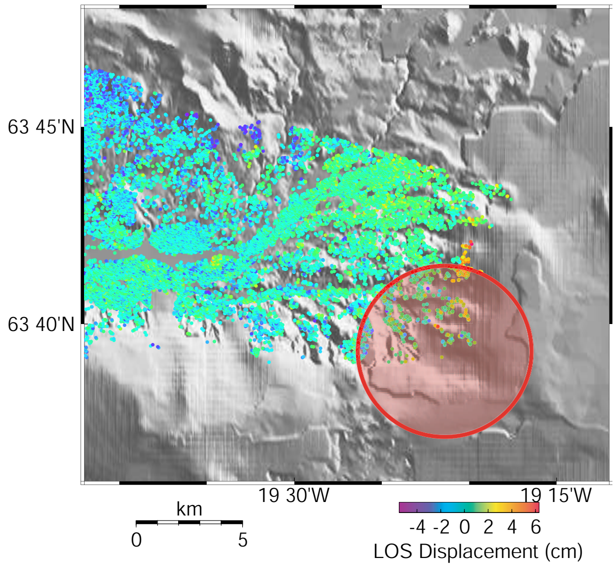

Figure 5. Displacement in the line-of-sight of persistent scatterer pixels to the west of Goðabunga area, between September 2000 and October 2003, from data acquired by ERS-2 satellite along track 324. Positive represents movement towards the satellite. The red shaded circle marks the approximate extent of the area of increased seismicity.

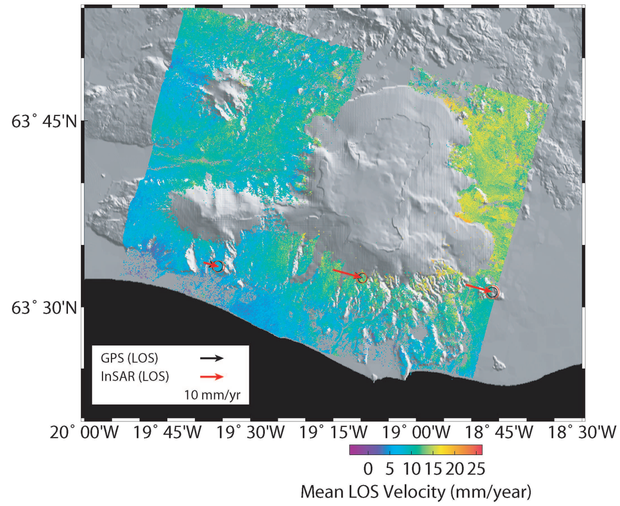

Figure 6. Mean line-of-sight velocities for stable InSAR pixels in a series of ERS images acquired along track 52 between 1995 and 1998. Positive represents movement towards the satellite. Also plotted in black are continuous GPS velocities relative to Reykjavík on the North American plate, projected into the satellite line-of-sight, with one sigma errors in the line-of-sight direction plotted as circles. For comparison line-of-sight velocities from stable InSAR pixels within 100 m of the GPS benchmark are plotted in red, with one sigma errors plotted as circles. The background image is topography in shaded relief.

4. DEFORMATION 1995 TO 1998

In order to determine the secular velocities on the flanks of Katla, we processed 16 images acquired between 1995 and 1998. We excluded ERS data acquired before and after this period to avoid including deformation due to two intrusive episodes in Eyjafjallajökull, one in 1994 and the other in 1999 to 2000. We used the combined multiple acquisition InSAR method of Hooper [14], which extracts the phase of both persistent scatterer pixels and stable distributed scatterer pixels using a high resolution small baseline approach.

The results are shown in Figure 6, together with the velocities of three continuous GPS stations projected into the satellite line-of-sight. There is an overall trend of increasing velocity towards the northeast, consistent with elastic and viscoelastc reponses expected due to thinning of the Vatnajökull ice cap, which lies to the northeast. There is also a trend of decreasing velocity radially outwards from Katla, consistent with the response to thinning of the Mýrdalsjökull ice cap overlaying Katla [15]. Also visible are variations in velocity on the flanks of Katla and Eyjafjallajökull, which may be due to creeping landslides.

5. CONCLUSIONS

Using an enhanced version of the method of Hooper et al. [11] we identify and unwrap the phase of persistent scatterer pixels using just eight images. Using the combined multiple acquisition InSAR approach of Hooper [14] we achieve better coverage than using the persistent scatterer method alone. We find that there is no significant systematic motion of the flanks of Katla from 1995 to 1998 and from 2000 to 2006, other than that expected from thinning of Vatnajökull and Mýrdalsjökull ice caps. We conclude that increased seismicity in the region of Goðbunga was not accompanied by significant deformation. We also detect local variations in velocities that may be due to landsliding.

ACKNOWLEDGMENTS

ENVISAT-ASAR and ERS data were provided by ESA under a Cat-1 proposal.

REFERENCES

[1] P. Einarsson and K. Sæmundsson. Earthquake epicenters 1982-1985 and volcanic systems in Iceland (map). In Th. Sigfússon, editor, *Í Hlutarsins Eðli: Festschrift for Thorbjorn Sigurgeirsson*. Menningarsjóður, Reykjavík, 1987.

[2] G. Larsen. Holocene eruptions within the Katla volcanic system, south Iceland: Characteristics and environmental impact. *Jökull*, 49:1–28, 2000.

[3] E. Sturkell, F. Sigmundsson, and P. Einarsson. Recent unrest and magma movements at Eyjafjallajökull and Katla volcanoes, Iceland. *J. Geophys. Res*, 108(B8), 2003.

[4] P. Einarsson. Atburðarás í tengslum við hlaup Š Jökulsá á Sólheimasandi í júlí 1999 (course of events associated with jökulhlaup in Jökulsá á Sólheimasandi in july 1999, abstract in Icelandic). *Geoscience Society of Iceland, Special Conference, Feb. 17, 2000, Abstract Volume*, page 14, 2000.

[5] K. S. Vogfjörð. Var eldgos orsök jarðskjálftaóróans í Sólheimajókulshlaupinu, 17 júlí 1999? (was volcanic tremor during the jökulhlaup from Sólheimajökull on 17 July 1999 caused by an eruption? in Icelandic). *Geoscience Society of Iceland, Abstract Volume*, page 32, 2002.

[6] M.T. Gudmundsson, Þ. Högnadóttir, H. Bjórnsson, and F. Pálsson. Jarðhitinn í Mýrdalsjökli og atburðirnir sumarið 1999 (geothermal activity beneath Mýrdalsjökull and the events of the summer of 1999, abstract in Icelandic). *Geoscience Society of Iceland, Special Conference, Feb. 17, 2000, Abstract Volume*, page 13, 2000.

[7] Erik Sturkell, Páll Einarsson, Matthew J. Roberts, Halldór Geirsson, Magnús Tumi Gudmundsson, Freysteinn Sigmundsson, Virginie Pinel, Gunnar B. Guðmundsson, Halldór Ólafsson, and Ragnar Stefánsson. Seismic and geodetic insights into magma accumulation at Katla subglacial volcano, Iceland: 1999 to 2005. in prep.

[8] Halldór Geirsson, Thóra Árnadóttir, Christof Völksen, Weiping Jiang, Erik Stukell, Thierry Villemin, Páll Einarsson, Freysteinn Sigmundsson, and Ragnar Stefánsson. Current plate movements across the Mid-Atlantic Ridge determined from 5 years of continous GPS measurements in Iceland. *J. Geophys. Res.*, 111:B09407, 2006.

[9] R. Pedersen and F. Sigmundsson. InSAR based sill model links spatially offset areas of deformation and seismicity for the 1994 unrest episode at Eyjafjallajökull volcano, Iceland. *Geophys. Res. Lett.*, 31:L14610, 2004.

[10] R. Pedersen and F. Sigmundsson. Temporal development of the 1999 intrusive episode in the Eyjafjallajökull volcano, Iceland, derived from InSAR images. *Bull. Volcanol.*, 68:377–393, 2006.

[11] A. Hooper, P. Segall, and H. Zebker. Persistent scatterer InSAR for crustal deformation analysis, with application to Volcán Alcedo, Galápagos. *J. Geophys. Res.*, (in press), 2007.

[12] A. Hooper and H. Zebker. Phase unwrapping in three dimensions with application to InSAR time series. *J. Opt. Soc. Amer. A*, in review.

[13] C. W. Chen. *Statistical-cost network-flow approaches to two-dimensional phase unwrapping for radar interferometry*. PhD thesis, Stanford University, 2001.

[14] A. Hooper. A combined multiple acquisition InSAR method incorporating both persistent scatterer and small baseline approaches. *Geophys. Res. Lett.*, in prep.

[15] V. Pinel, F. Sigmundsson, E. Stukell, H. Geirsson, P. Einarsson, M.T. Gudmundsson, and T. Högnadóttir. Discriminating volcano deformation due to magma movements and variable surface loads: Application to Katla subglacial volcano, Iceland. *Geophys. J. Int.*, 169:325–338, 2007.